Inorganic Chemistry

Article

pubs.acs.org/IC

Partial Nitrogen Atom Transfer: A New Synthetic Tool to Design Single-Molecule Magnets

Mei Ding,[†] Mathieu Rouzières,[‡,§] Yaroslav Losovyj,[†] Maren Pink,[†] Rodolphe Clérac,*[,‡,§] and Jeremy M. Smith*[,†]

[†]Department of Chemistry, Indiana University, 800 E. Kirkwood Avenue, Bloomington, Indiana 47405, United States

[‡]CNRS, CRPP, UPR 8641, F-33600 Pessac, France

[§]Univ. Bordeaux, CRPP, UPR 8641, F-33600 Pessac, France

Supporting Information

ABSTRACT: Incomplete nitrogen atom transfer from the iron(IV) nitride complex $PhB(MesIm)_3Fe{\equiv}N$ to the vanadium(III) complex $V(Mes)_3(THF)$ quantitatively provides the bimetallic complex $PhB(MesIm)_3Fe\text{-}N{=}V(Mes)_3$. Structural and spectroscopic characterizations reveal that the nitride ligand forms a linear bridge between V(V) and high-spin Fe(II) metal ions, confirming that atom transfer is accompanied by electron transfer. In the presence of an applied dc field, the complex displays slow relaxation of the magnetization, revealing its single-molecule magnet properties with an estimation of the energy barrier at about 10 K. This complex establishes a synthetic principle for the assembly of paramagnetic complexes bridged by nitride ligands.

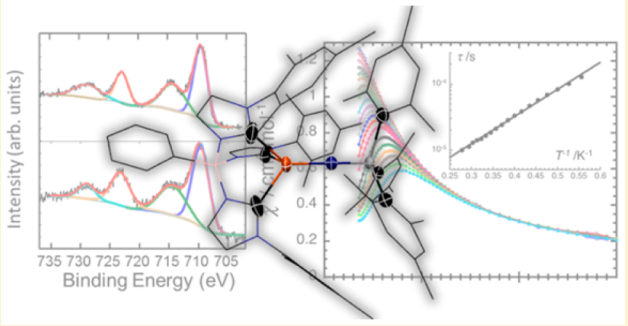

INTRODUCTION

Single-molecule magnets (SMMs) were discovered over two decades ago, when it was observed that certain paramagnetic molecules can behave as classical bulk magnets at low temperature, i.e., by retaining their magnetization during a characteristic time upon removal of an applied external field. Part of the interest driving the study of SMMs is their potential for application in nanoscale magnetic devices, including high-density spin-based information storage and processing,[1] spintronics,[2] and quantum computing.[3]

The magnet-like behavior in an SMM originates from an energy barrier to its spin reversal (Δ) that depends on the ground spin state (S_T) and uniaxial zero-field splitting parameter (D), $\Delta = |D|S_T^2$ for integer spins, $\Delta = |D|(S_T^2 - 1/4)$ for half-integer spins (with $H = DS_{Tz}^2$).[4] One strategy for synthesizing SMMs is to prepare polynuclear complexes that maximize S_T; however, the rational synthesis of such species is challenging.[5] Well-defined complexes can be constructed by a modular approach in which discrete metal-containing building blocks are linked by bridging ligands.[6] While the predictable chemistry of the cyanide ligand has resulted in the building block approach being dominated by this linker,[6,7] other linking groups are known. For example, multinuclear oxo-bridged complexes have been prepared from diamagnetic transition-metal oxo complexes and suitable lanthanide synthons; however, these assembly reactions do not involve electron transfer and the SMM properties arise solely from the lanthanide component.[6,8] Given our interests in nitrogen atom transfer chemistry,[9] we were intrigued by the idea of extending this synthetic strategy to partial nitrogen atom transfer, where the electron transfer associated with atom transfer would both generate a single atom linker as well as unveil SMM behavior.

While both two- and three-electron nitrogen atom transfer reactions can be used to prepare new nitride complexes,[10] e.g., from (salen)Mn≡N and its derivatives,[11] with appropriately chosen precursors, it is possible to prevent complete transfer of the nitrogen atom, resulting in the formation of dinuclear nitride-bridged complexes. For example, OsO_3N reacts with a number of metal complexes to form binuclear compounds, e.g., $Ru(CO)(Et_2dtc)(PPh_3)_2NOsO_3$ (Et_2dtc = *N*,*N*-diethyldithiocarbamate).[12] However, these products are best viewed as Lewis acid−base adducts in which there is no electron transfer between the two metal ions.[13,14]

In previous work, we have shown that iron(IV) nitride complexes supported by tripodal tris(carbene)borate ligands participate in two-electron nitrogen atom transfer reactions to a range of substrates.[9] Specifically, these complexes react with a range of small molecules, including phosphines,[15] CN^tBu,[16] CO,[16] dienes,[17] and styrenes,[18] typically, to afford new high-spin ferrous complexes in which the functionalized substrate is bound to iron (Scheme 1). On the basis of these considerations, we were intrigued by the possibility that a

Received: June 28, 2015
Published: August 31, 2015

DOI: 10.1021/acs.inorgchem.5b01455
Inorg. Chem. 2015, 54, 9075−9080

Scheme 1

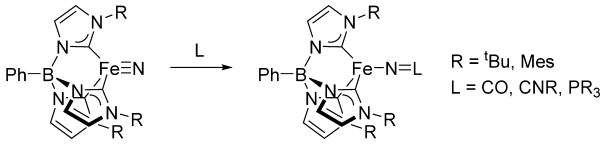

dinuclear complex could be assembled by a two-electron nitrogen atom transfer reaction from an iron(IV) nitride to a suitable substrate complex. We anticipated that, with the steric protection provided by the bulky tris(carbene)borate ligand, assembly of such a dinuclear complex would be well-controlled.

In addition to these synthetic considerations, the magnetic properties of ferrous tris(carbene)borate complexes also gave us confidence that a nitride-bridged dinuclear complex would be a good candidate for SMM behavior. For example, at temperatures below 5 K, the photoexcited high-spin state of $PhB(MesIm)_3Fe\text{-}N{=}PPh_3$[19] shows single-molecule magnet properties revealed by applying a dc field,[20] suggesting that the environment engendered by the tris(carbene)borate ligand may facilitate slow relaxation of the magnetization for the high-spin iron(II) metal ion.

In this work, we report the successful synthesis of a paramagnetic binuclear complex that is formed by a partial nitrogen atom transfer reaction. Structural and spectroscopic studies reveal that assembly of the complex is accompanied by a two-electron transfer reaction. This electron transfer creates a magnetically anisotropic metal center, which, in turn, leads to single-molecule magnet properties. While further improvements to the complex design can be envisioned, this result provides proof-of-concept that partial nitrogen atom transfer concomitant with electron transfer represents a viable strategy to assemble multinuclear single-molecule magnets.

EXPERIMENTAL SECTION

All manipulations were performed under a nitrogen atmosphere by standard Schlenk techniques or in an MBraun Labmaster glovebox. Glassware was dried at 150 °C overnight. Diethyl ether, *n*-pentane, tetrahydrofuran, and toluene were purified by the Glass Contour solvent purification system. Deuterated benzene was first dried with CaH_2, then over Na/benzophenone, and then vacuum transferred into a storage container. Before use, an aliquot of each solvent was tested with a drop of sodium benzophenone ketyl in THF solution. The complexes $PhB(MesIm)_3Fe{\equiv}N$[21] and $V(Mes)_3(THF)$[22] were prepared according to literature procedures. ^{1}H NMR data were recorded on a Varian Inova 400 MHz spectrometer at 20 °C. Resonances in the ^{1}H NMR spectra are referenced to residual THF-d_8 at either δ = 3.58 or 1.76 ppm. UV−visible spectra were recorded on an Agilent Cary 60 UV−vis spectrophotometer equipped with a Unisoku cryostat. Elemental analysis data were collected by Midwest Microlab, LLC (Indianapolis, IN).

Synthesis of $PhB(MesIm)_3Fe\text{-}N{=}V(Mes)_3$ (1). Blue $V(Mes)_3(THF)$ (200 mg, 0.28 mmol) and orange $PhB(MesIm)_3Fe{\equiv}N$ (134.6 mg, 0.28 mmol) were mixed in THF at room temperature (10 mL). The resulting brown solution was stirred at room temperature overnight. The solvent was removed *in vacuo* to obtain a brown solid. The complex was crystallized by slow diffusion of *n*-pentane into a THF solution of the product at −35 °C (52% yield). ^{1}H NMR (C_6D_6): δ 65.3 (3H), 61.8 (3H), 46.8 (2H), 27.7 (9H), 23.1 (2H), 19.9 (1H), 13.3 (3H), 9.3 (9H), 5.51 (3H), −0.45 (9H), −3.6 (3H), −4.7 (3H), −29.8 (9H), −43.3 (9H). ^{1}H NMR (THF-d_8): δ 58.7 (3H), 58.3 (2H), 41.4 (3H), 23.9 (9H), 21.1 (2H), 18.3 (1H), 12.1 (3H), 8.5 (9H), 7.4 (2H), −0.1 (9H), −2.5 (3H), −3.1 (3H), −25.3 (9H), −36.8 (9H). UV−vis (C_7H_8) λ_{max}, nm (ε, $M^{-1}cm^{-1}$): 289 (14700), 343 (16850). Anal. Calcd for $C_{69}H_{77}BFeN_7V$: C, 73.86; H, 7.19; N, 8.36. Found: C, 73.86; H, 6.92; N, 8.74.

X-ray Photoelectron Spectroscopy. XPS experiments were performed using a PHI Versa Probe II instrument equipped with a monochromatic Al Kα source. The X-ray power of 25 W at 15 kV was used for a 100 μm beam size. The instrument work function was calibrated to give a binding energy (BE) of 84.0 eV for the Au $4f_{7/2}$ line for metallic gold, and the spectrometer dispersion was adjusted to give BEs of 284.8, 932.7, and of 368.3 eV for the C 1s line of adventitious (aliphatic) carbon presented on the nonsputtered samples, Cu $2p_{3/2}$ and Ag $3d_{5/2}$ photoemission lines, respectively. The PHI double charge compensation system was used on all samples. The ultimate Versa Probe II instrumental resolution was determined to be better than 0.125 eV using the Fermi edge of the valence band for metallic silver. XPS spectra with the energy step of 0.1 eV were recorded using the software SmartSoft−XPS v2.0 and processed using PHI MultiPack v9.0 and/or CasaXPS v.2.3.14 at the pass energies of 46.95, 23.5, and 11.75 eV for Fe and V 2p, N 1s, C 1s regions, respectively. Peaks were fitted using GL line shapes, i.e., a combination of Gaussians and Lorentzians with 0−50% of Lorentzian contents. Shirley background was used for curve-fitting.

A PHI Versa Probe II special vessel was used for sample transfer from the inert atmosphere glovebox to the XPS chamber. The XPS samples were prepared by drop-casting on the clean native surface of the Si(111) wafer.

Magnetometry. The magnetic measurements were carried out with the use of a Quantum Design MPMS-XL SQUID magnetometer and PPMS-9 susceptometer. These instruments work between 1.8 and 400 K with applied dc fields ranging from −7 to 7 T (MPMS). Measurements were performed on a polycrystalline sample of **1** (17.9 mg) sealed in a polyethylene bag (3 × 0.5 × 0.02 cm; 35.2 mg) and covered with mineral oil (7.0 mg). Prior to the experiments, the field-dependent magnetization was measured at 100 K in order to detect the presence of any bulk ferromagnetic impurities. The sample appeared to be free of any significant ferromagnetic impurities. ac susceptibility measurements were made with an oscillating field of 1 Oe with a frequency from 10 to 10 000 Hz (PPMS). The magnetic data were corrected for the sample holder, mineral oil, and the intrinsic diamagnetic contributions.

RESULTS AND DISCUSSION

The previously reported iron(IV) nitride complex, $PhB(MesIm)_3Fe{\equiv}N$,[21] reacts cleanly with $V(Mes)_3(THF)$, a synthon for three-coordinate V(III),[22] to yield the heterobimetallic complex $PhB(MesIm)_3Fe\text{-}N{=}V(Mes)_3$ **1** in high yield (Scheme 2). Complex **1** has been structurally

Scheme 2

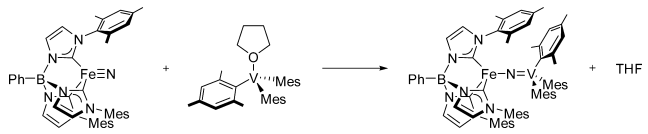

characterized (Figure 1), revealing the desired structure with the iron and vanadium ions connected by a linear nitride bridge. Both metals are in local 3-fold symmetric environments, with the $V(Mes)_3$ unit adopting a staggered conformation relative to the iron tris(carbene)borate unit.

The structural metrics suggest that the complex contains a high-spin (S = 2) iron(II) center. Specifically, the Fe−C bond lengths (2.176(6) Å) are the same as those observed for other high-spin iron(II) tris(carbene)borate complexes[15,16,18,20] and longer than those observed in low-spin iron(II) tris(carbene)-borate complexes.[18] Consistent with a high-spin state, the Fe−N bond length (1.953(7) Å) is similar to what is observed in four-coordinate iron amido complexes (average = 1.94(5) Å),[23]

DOI: 10.1021/acs.inorgchem.5b01455
Inorg. Chem. 2015, 54, 9075−9080

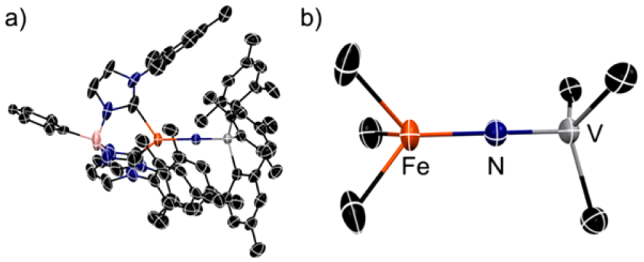

Figure 1. Molecular structure of **1**, thermal ellipsoids shown at 50% probability, hydrogen atoms omitted for clarity. (a) Full complex. (b) Expansion of the Fe−N−V core in **1**. Selected bond lengths and angles: Fe−N 1.953(7) Å; V−N 1.625(7) Å; Fe−N−V 180.0°.

but longer than what is observed for low-spin iron(II) imido[20,24] or phosphoriminato[18] complexes. In addition, the Fe−N bond distance is significantly longer than those observed for iron(III) or iron(IV) imido complexes in 3-fold symmetry.[25] The structural metrics around the vanadium center are less informative. Although the V−N bond length (1.625(7) Å) is among the shortest reported for four-coordinate vanadium(V) imido complexes,[26] the V−C bond lengths (2.094(5) Å) are longer than those observed for O═V(Mes)$_3$[27] (2.025−2.077 Å) but shorter than those for the V(III) starting material (THF)V(Mes)$_3$ (2.095−2.117 Å).[21] While these longer V−C bond lengths may be a consequence of the greater steric congestion in **1**, electronic factors cannot be eliminated at this stage.

Thus, while the weight of the structural data is most consistent with an Fe(II)/V(V) formulation, a number of other oxidation states are possible, including Fe(III)/V(IV) and Fe(IV)/V(III). We have, therefore, used X-ray photoelectron spectroscopy (XPS) to assign oxidation states for the iron and vanadium centers in complex **1**. XPS determines the photoelectron binding energy (BE) of atoms in a molecule.[28] The photoelectron BEs are atom-specific and sensitive to the chemical environment, thus providing information on atomic oxidation states. Internally consistent oxidation state assignments can be made since the XPS of multiple elements can be measured in a single sample. To provide appropriate reference points for the binding energies (BEs) of complex **1**, we also measured XPS for two related compounds where the oxidation state of the metal is unambiguous, namely, the vanadium(V) complex O═V(Mes)$_3$[26] and the iron(II) complex PhB(MesIm)$_3$FeCl.[29] Reassuringly, the BEs of these two complexes are consistent with previous literature reports for bulk materials (Figure 2, Tables S1 and S3). Specifically, for O═V(Mes)$_3$, the 2p$_{3/2}$ binding energy (516.95 eV) is consistent with that reported for a fresh in-vacuum cleaved V_2O_5(001) surface[30,31] and for thin vanadium oxide films,[32] whereas, for PhB(MesIm)$_3$FeCl, the binding energy of the 2p$_{3/2}$ line (709.35 eV) and the BE of the shake-up satellite (714.74 eV) are consistent with the values reported for Fe^{2+} ions in bulk materials.[33,34] The spin−orbit couplings for the 2p region of both complexes (Tables S1 and S3) perfectly match previously reported results.[29−31,35]

The binding energies for the V 2p$_{3/2}$ (515.91 eV) as well as Fe 2p$_{3/2}$ line (709.65 eV) and shake-up satellite (714.39 eV) in the bimetallic complex **1** are consistent with those of the reference compounds. Thus, on the basis of the XPS data, we assign oxidation states of +2 to iron and +5 to vanadium in complex **1**, i.e., PhB(MesIm)$_3$Fe^{II}-N═V^{V}(Mes)$_3$, in agreement with the structural data. Minor differences in the BEs as well as

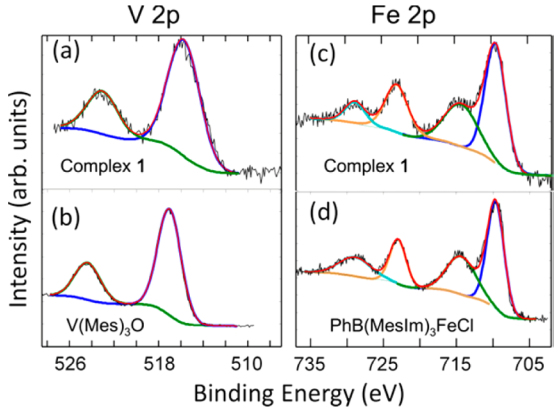

Figure 2. High-resolution V 2p spectra of (a) bimetallic complex **1** and (b) O═V(Mes)$_3$ reference sample. The black line represents the experimental data, the red line shows the generated fit, and the blue line and green line represent V 2p$_{3/2}$ and V 2p$_{1/2}$ components, correspondingly. See Table S1 for fitting parameters. High-resolution Fe 2p spectra of (c) bimetallic complex **1** and (d) PhB(MesIm)$_3$FeCl. The black line represents the experimental data, the red line shows generated fit, and the blue line and yellow line represent Fe 2p$_{3/2}$ and Fe 2p$_{1/2}$ components, correspondingly. Green and cyan show shake-up satellites. See Table S3 for fitting parameters.

the broadening of the V 2p$_{3/2}$ line are attributed to the greater covalency of these complexes than in the bulk reference materials, as well as possible charge delocalization between the metals in complex **1**.[36]

The magnetic properties of **1** have been studied by dc and ac techniques. The room-temperature χT product of the isolated complex **1** is 3.9 cm^3 K/mol (Figure 3), in good agreement

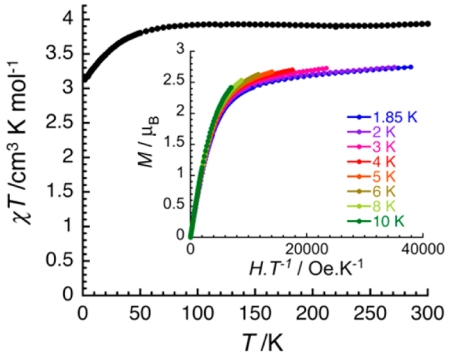

Figure 3. Temperature dependence of χT at 1000 Oe (χ is defined as molar magnetic susceptibility equal to M/H per mole of **1**) for a polycrystalline sample of **1**. Inset: M vs H/T data for **1** (50−300 Oe min^{-1}).

with a magnetically isolated high-spin (S = 2, g = 2.28(5)) iron(II) center, as suggested by the structural data (vide supra). The geometric and electronic structure of the iron center suggests that it is likely to have significantly strong magnetic anisotropy, similar to other four-coordinate iron(II) complexes in 3-fold symmetry.[37] The effect of the magnetic anisotropy is clearly seen by the decrease of the χT product when lowering the temperature (Figure 3) and by the absence of saturation of the magnetization even at 1.85 K and under 7 T (2.8 μ_B; inset, Figure 3). This consideration prompted us to investigate the magnetization dynamics of this complex. In the absence of a dc field, there is no out-of-phase component above 1.8 K in the ac susceptibility for frequencies up to 10 kHz. However,

DOI: 10.1021/acs.inorgchem.5b01455
Inorg. Chem. 2015, 54, 9075−9080

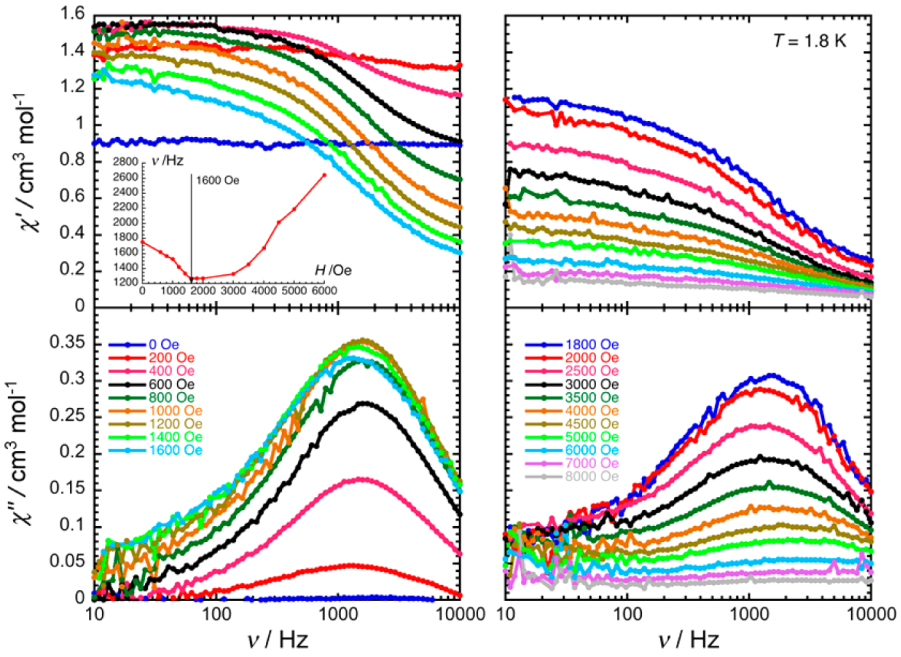

Figure 4. Frequency dependence of the real (χ', top) and imaginary (χ'', bottom) parts of the ac susceptibility at 1.8 K with different ac frequencies between 10 and 10000 Hz and different dc fields between 0 and 8000 Oe for a polycrystalline sample of **1**. Solid lines are guides. Inset: Field dependence of the characteristic ac frequencies of the relaxation mode from the main figure. Solid lines are visual guides.

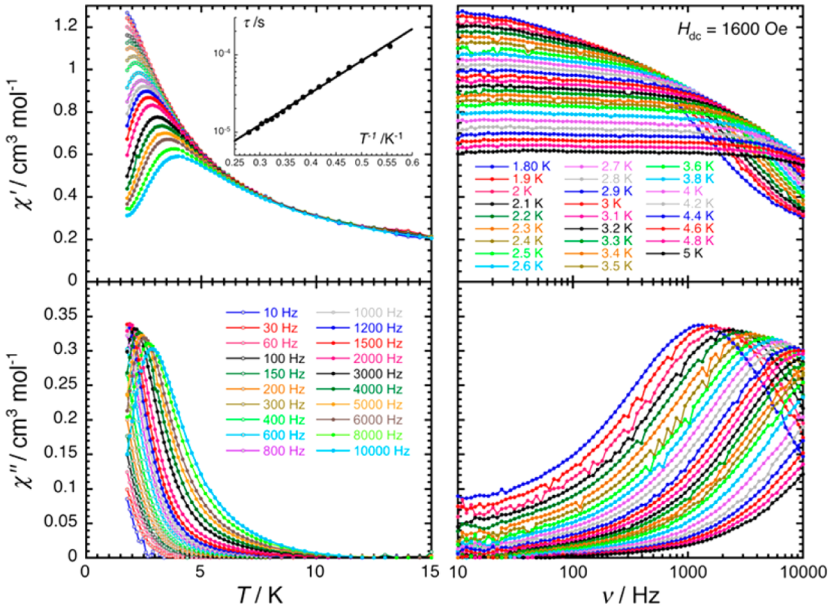

Figure 5. Temperature (left) and frequency (right) dependence of the real (χ', top) and imaginary (χ'', bottom) parts of the ac susceptibility, between 10 and 10 000 Hz and between 1.8 and 15 K, respectively, for **1** in 1600 Oe dc field. Solid lines are visual guides. Inset: τ vs T^{-1} plot for **1** in 1600 Oe dc field. The black solid line corresponds to the least-squares fit of the data to an Arrhenius law (see text).

application of a dc field leads to the detection of a single mode out-of-phase signal (Figure 4), revealing the slow dynamics of the magnetization of **1**.

The field dependence of the characteristic relaxation frequency at 1.8 K reveals that the relaxation time, τ, is maximum for an optimum applied dc field of 1600 Oe (inset, Figure 4), indicating a competition between the thermally activated and quantum tunneling pathways of magnetization relaxation. Variable-frequency ac susceptibility data were thus collected under 1600 Oe between 1.8 and 15 K (Figure 5) to determine the temperature dependence of the relaxation time. From these data, the τ vs T^{-1} plot was constructed (inset, Figure 5), demonstrating the thermal activation of the relaxation time (i.e., it follows an Arrhenius law) with a pre-exponential factor, τ_0, of 7.1×10^{-7} s and an energy gap of 9.5(5) K (6.6 cm^{-1}, which gives a lower bound of the D parameter of −2.4 K or −1.7 cm^{-1}).

CONCLUSION

Two-electron nitrogen atom transfer from an iron(IV) nitride to a vanadium(III) substrate leads to the formation of the binuclear complex $PhB(MesIm)_3Fe\text{-}N{=}V(Mes)_3$ **1**, in which

DOI: 10.1021/acs.inorgchem.5b01455
Inorg. Chem. 2015, 54, 9075−9080

the two metals are linked by a nitride bridge. Structural and spectroscopic characterizations of **1** demonstrate that the complex contains a high-spin (S = 2) iron(II) center that displays SMM properties revealed in the presence of an applied dc field.[38] Importantly, the preparation of complex **1** establishes partial nitrogen atom transfer as a strategy for the well-controlled synthesis of magnetic polynuclear complexes. Since the short and highly covalent nitride bridge should allow for strong magnetic coupling between paramagnetic centers,[23,39] partial nitrogen atom transfer may allow for the rational assembly of larger complexes that are akin to cyanide-linked complexes,[7] but featuring stronger intramolecular exchange between appropriate magnetic centers. While such species are not accessible from **1**, as evidenced by the lack of reversible waves in the cyclic voltammogram of complex **1**, other low coordinate synthons are expected to provide complexes in which a nitride links two paramagnetic ions. Investigations aimed at exploring this synthetic strategy are currently underway.

■ ASSOCIATED CONTENT

Supporting Information

The Supporting Information is available free of charge on the ACS Publications website at DOI: 10.1021/acs.inorgchem.5b01455.

Additional experimental information (PDF)

Additional crystallographic data (CIF)

■ AUTHOR INFORMATION

Corresponding Authors

*E-mail: clerac@crpp-bordeaux.cnrs.fr (R.C.).

*E-mail: smith962@indiana.edu (J.M.S.).

Author Contributions

All authors have given approval to the final version of the manuscript.

Notes

The authors declare no competing financial interests.

■ ACKNOWLEDGMENTS

M.D. and J.M.S. acknowledge funding from Indiana University and the NSF (CHE-1112299). ChemMatCARS Sector 15 is principally supported by the National Science Foundation/Department of Energy under grant number NSF/CHE-1346572. Use of the Advanced Photon Source was supported by the DOE-BES (DE-AC02-06CH11357). R.C. and M.R. thank the University of Bordeaux, the ANR, the Conseil Régional d'Aquitaine, and the CNRS for financial support. The XPS was funded by the NSF (DMR MRI-1126394). We thank the IU Nanoscale Characterization Facility for access to this instrument.

■ REFERENCES

(1) Ardavan, A.; Blundell, S. J. *J. Mater. Chem.* **2009**, *19*, 1754−1760.

(2) (a) Rocha, A. R.; García-Suárez, V. M.; Bailey, S. W.; Lambert, C. J.; Ferrer, J.; Sanvito, S. *Nat. Mater.* **2005**, *4*, 335−339. (b) Bogani, L.; Wernsdorfer, W. *Nat. Mater.* **2008**, *7*, 179−186.

(3) (a) Leuenberger, M. N.; Loss, D. *Nature* **2001**, *410*, 789−793. (b) Stamp, P. C. E.; Gaita-Ariña, A. *J. Mater. Chem.* **2009**, *19*, 1718−1730.

(4) Gatteschi, D.; Sessoli, R.; Villain, J. *Molecular Nanomagnets*; Oxford University Press: Oxford, U.K., 2006.

(5) Aromí, G.; Brechin, E. K. *Struct. Bonding (Berlin, Ger.)* **2006**, *122*, 1−67.

(6) Pedersen, K. S.; Bendix, J.; Clérac, R. *Chem. Commun.* **2014**, *50*, 4396−4415.

(7) Recent reviews: (a) Beltran, L. M. C.; Long, J. R. *Acc. Chem. Res.* **2005**, *38*, 325−334. (b) Atanasov, M.; Comba, P.; Hausberg, S.; Martin, B. *Coord. Chem. Rev.* **2009**, *253*, 2306−2314. (c) Shatruk, M.; Avendano, C.; Dunbar, K. *Prog. Inorg. Chem.* **2009**, *56*, 155−334. (d) Wang, S.; Ding, X.-H.; Zuo, J.-L.; You, X.-Z.; Huang, W. *Coord. Chem. Rev.* **2011**, *255*, 1713−1732. (e) Wang, S.; Ding, X.-H.; Li, Y.-H.; Huang, W. *Coord. Chem. Rev.* **2012**, *256*, 439−464. (f) Li, Y.-H.; He, W.-R.; Ding, X.-H.; Wang, S.; Cui, L.-F.; Huang, W. *Coord. Chem. Rev.* **2012**, *256*, 2795−2815.

(8) (a) Pointillart, F.; Bernot, K.; Sessoli, R. *Inorg. Chem. Commun.* **2007**, *10*, 471−474. (b) Pointillart, F.; Bernot, K.; Sessoli, R.; Gatteschi, D. *Inorg. Chem.* **2010**, *49*, 4355−4361. (c) Pedersen, K. S.; Dreiser, J.; Schau-Magnussen, M.; Thuesen, C. A.; Weihe, H.; Bendix, J. *Polyhedron* **2012**, *46*, 47−52.

(9) Recent reviews: (a) Smith, J. M.; Subedi, D. *Dalton Trans.* **2012**, *41*, 1423−1429. (b) Smith, J. M. *Prog. Inorg. Chem.* **2014**, *58*, 417−470.

(10) Woo, L. K. *Chem. Rev.* **1993**, *93*, 1125−1136.

(11) (a) Du Bois, J.; Hong, J.; Carreira, E. M.; Day, M. W. *J. Am. Chem. Soc.* **1996**, *118*, 915−916. (b) Golubkov, G.; Gross, Z. *Angew. Chem., Int. Ed.* **2003**, *42*, 4507−4510. (c) Bendix, J. *J. Am. Chem. Soc.* **2003**, *125*, 13348−13349.

(12) Zheng, H.; Leung, W.-H.; Chim, J. L. C.; Lai, W.; Lam, C.-H.; Williams, I. D.; Wong, W.-T. *Inorg. Chim. Acta* **2000**, *306*, 184−192.

(13) Paramagnetic complexes formed by partial nitrogen atom transfer are known; however, electron transfer does not occur. See, for example: (a) Morrogh, D.; Galceran Mestres, M.; Niquet, E.; Barboza da Silva, C. F.; Santos Saez, A.; Schwarz, S.; Strähle, J. *Z. Anorg. Allg. Chem.* **2005**, *631*, 1113−1118. (b) Hedegaard, E. D.; Schau-Magnussen, M.; Bendix, J. *Inorg. Chem. Commun.* **2011**, *14*, 719−721. (c) Bendix, J.; Anthon, C.; Schau-Magnussen, M.; Brock-Nannestad, T.; Vibenholt, J.; Rehman, M.; Sauer, S. P. A. *Angew. Chem., Int. Ed.* **2011**, *50*, 4480−4483.

(14) Low-spin nitride-bridged diiron complexes are believed to be formed by nitrogen atom transfer: (a) Brown, S. D.; Peters, J. C. *J. Am. Chem. Soc.* **2005**, *127*, 1913−1923. (b) Brown, S. D.; Mehn, M. P.; Peters, J. C. *J. Am. Chem. Soc.* **2005**, *127*, 13146−13147.

(15) (a) Scepaniak, J. J.; Fulton, M. D.; Bontchev, R. P.; Duesler, E. N.; Kirk, M. L.; Smith, J. M. *J. Am. Chem. Soc.* **2008**, *130*, 10515−10517. (b) Scepaniak, J. J.; Margarit, C. G.; Harvey, J. N.; Smith, J. M. *Inorg. Chem.* **2011**, *50*, 9508−9517.

(16) Scepaniak, J. J.; Bontchev, R. P.; Johnson, D. L.; Smith, J. M. *Angew. Chem., Int. Ed.* **2011**, *50*, 6630−6633.

(17) Lee, W.-T.; Juarez, R. A.; Scepaniak, J. J.; Muñoz, S. B.; Dickie, D. A.; Wang, H.; Smith, J. M. *Inorg. Chem.* **2014**, *53*, 8425−8430.

(18) Muñoz, S. B., III; Lee, W.-T.; Dickie, D. A.; Scepaniak, J. J.; Subedi, D.; Pink, M.; Johnson, M. D.; Smith, J. M. *Angew. Chem., Int. Ed.* **2015**, *54*, ASAP article. DOI: 10.1002/anie.201503773.

(19) (a) Scepaniak, J. J.; Harris, T. D.; Vogel, C. S.; Sutter, J.; Meyer, K.; Smith, J. M. *J. Am. Chem. Soc.* **2011**, *133*, 3824−3827. (b) Lin, H.-J.; Siretanu, D.; Dickie, D. A.; Subedi, D.; Scepaniak, J. J.; Mitcov, D.; Clérac, R.; Smith, J. M. *J. Am. Chem. Soc.* **2014**, *136*, 13326−13332.

(20) Mathonière, C.; Lin, H.-J.; Siretanu, D.; Clérac, R.; Smith, J. M. *J. Am. Chem. Soc.* **2013**, *135*, 19083−19086.

(21) Scepaniak, J. J.; Young, J. A.; Bontchev, R. P.; Smith, J. M. *Angew. Chem., Int. Ed.* **2009**, *48*, 3158−3160.

(22) (a) Seidel, W.; Kreisel, G. *Z. Anorg. Allg. Chem.* **1977**, *435*, 146−152. (b) Vivanco, M.; Ruiz, J.; Floriani, C.; Chiesi-Villa, A.; Rizzoli, C. *Organometallics* **1993**, *12*, 1794−1801.

(23) See the Supporting Information for a listing of structurally characterized Fe(II) amido complexes.

(24) Brown, S. D.; Peters, J. C. *J. Am. Chem. Soc.* **2005**, *127*, 1913−1923.

(25) See the Supporting Information for a listing of iron imido complexes in 3-fold symmetry.

DOI: 10.1021/acs.inorgchem.5b01455
Inorg. Chem. 2015, 54, 9075−9080

(26) (a) Nugent, W. A.; Harlow, R. L. *J. Chem. Soc., Chem. Commun.* **1979**, 342−343. (b) Zhang, W.; Nomura, K. *Inorg. Chem.* **2008**, *47*, 6482−6492.
(27) (a) Ruiz, J.; Vivanco, M.; Floriani, C.; Chiesi-Villa, A.; Guastini, C. *J. Chem. Soc., Chem. Commun.* **1991**, 762−764. (b) Vivanco, M.; Ruiz, J.; Floriani, C.; Chiesi-Villa, A.; Rizzoli, C. *Organometallics* **1993**, *12*, 1802−1810.
(28) Turner, D. W.; Jobory, M. I. A. *J. Chem. Phys.* **1962**, *37*, 3007−3008.
(29) Nieto, I.; Ding, F.; Bontchev, R. P.; Wang, H.; Smith, J. M. *J. Am. Chem. Soc.* **2008**, *130*, 2716−2717.
(30) Silversmit, G.; Depla, D.; Poelman, H.; Marin, G. B.; De Gryse, R. *Surf. Sci.* **2006**, *600*, 3512−3517.
(31) Silversmit, G.; Depla, D.; Poelman, H.; Marin, G. B.; De Gryse, R. *J. Electron Spectrosc. Relat. Phenom.* **2004**, *135*, 167−175.
(32) Chen, Y.; Xie, K.; Liu, Z. *Appl. Surf. Sci.* **1998**, *126*, 347−351.
(33) Yamashita, T.; Hayes, P. *Appl. Surf. Sci.* **2008**, *254*, 2441−2449.
(34) The spectra of other possible oxidation states (V^{4+} and Fe^{3+}) are reported to be at lower (515.8 eV for V^{4+}) and higher (711.0 eV for Fe^{3+} $2p_{3/2}$ and 718.8 eV for satellite Fe^{3+} feature) energies; see refs 30, 31, 32, and 35.
(35) Mendialdua, J.; Casanova, R.; Barbaux, Y. *J. Electron Spectrosc. Relat. Phenom.* **1995**, *71*, 249−261.
(36) Additional discussion of the XPS data is provided in the Supporting Information.
(37) (a) Freedman, D. E.; Harman, W. H.; Harris, T. D.; Long, G. J.; Chang, C. J.; Long, J. R. *J. Am. Chem. Soc.* **2010**, *132*, 1224−1225. (b) Harman, W. H.; Harris, T. D.; Freedman, D. E.; Fong, H.; Chang, A.; Rinehart, J. D.; Ozarowski, A.; Sougrati, M. T.; Grandjean, F.; Long, G. J.; Long, J. R.; Chang, C. J. *J. Am. Chem. Soc.* **2010**, *132*, 18115−18126. (c) Weismann, D.; Sun, Y.; Lan, Y.; Wolmershäuser, G.; Powell, A. K.; Sitzmann, H. *Chem.−Eur. J.* **2011**, *17*, 4700−4704.
(38) For examples of other organometallic single-molecule magnets, see: Layfield, R. A. *Organometallics* **2014**, *33*, 1084−1099.
(39) See, for example: (a) Bottomley, L. A.; Garrett, B. B. *Inorg. Chem.* **1982**, *21*, 1260−1263. (b) Kadish, K. M.; Bottomley, L. A.; Brace, J. G.; Winograd, N. *J. Am. Chem. Soc.* **1980**, *102*, 4341−4344. (c) Jüstel, T.; Müller, M.; Weyhermüller, T.; Kressl, C.; Bill, E.; Hildebrandt, P.; Lengen, M.; Grodzicki, M.; Trautwein, A. X.; Nuber, B.; Wieghardt, K. *Chem.—Eur. J.* **1999**, *5*, 793−810. (d) Dutta, S. K.; Beckmann, U.; Bill, E.; Weyhermüller, T.; Wieghardt, K. *Inorg. Chem.* **2000**, *39*, 3355−3364.

DOI: 10.1021/acs.inorgchem.5b01455
Inorg. Chem. 2015, 54, 9075−9080